The AAPS Journal (2019) 21: 86
DOI: 10.1208/s12248-019-0345-7

Research Article

Theme: Natural Products Drug Discovery in Cancer Prevention
Guest Editors: Ah-Ng Tony Kong and Chi Chen

A Tangeretin Derivative Inhibits the Growth of Human Prostate Cancer LNCaP Cells by Epigenetically Restoring p21 Gene Expression and Inhibiting Cancer Stem-like Cell Proliferation

Guor-Jien Wei,[1] Yen-Hsiang Chao,[2] Yen-Chen Tung,[3] Tien-Yuan Wu,[4] and Zheng-Yuan Su[2,5]

Received 16 January 2019; accepted 27 May 2019; published online 10 July 2019

Abstract. Prostate cancer ranks the second in incidence and the fifth in mortality cancer in male globally. Citrus polymethoxyflavonoids (PMFs), such as tangeretin (PMF1), have been found to exhibit various biological activities. Here, we evaluated the inhibitory effects and mechanism of synthetic 5,4′-didemethyltangeretin (PMF2) on human prostate cancer LNCaP cells. We found that PMF2 inhibited the growth of LNCaP cells (GI_{50} 14.6 μM) more strongly than PMF1, and it was less cytotoxic against the normal human prostate RWPE-1 cells. PMF2 upregulated Bad and Bax, downregulated Bcl-2, and activated caspase-3 and PARP in the LNCaP cells, thereby inducing apoptosis. PMF2 also suppressed the anchorage-independent growth of the LNCaP cells. It triggered p21 gene expression by demethylation of the p21 promoter region, and inhibited the protein expressions of DNMT 3B and HDACs 1, 2, and 4/5/9 by epigenetic regulations. We further found that PMF2 showed interactions with DNMTs 1, 2, and 3A *ex vivo*, which might inhibit DNMT activity. Additionally, PMF2 decreased the anchorage-independent growth of isolated LNCaP cancer stem-like cells (CSLCs) with high CD166 mRNA expression. These results indicated that PMF2 might inhibit the growth of human prostate cancer cells through different mechanisms, suggesting that PMF2 could be an innovative agent for prostate cancer therapy and prevention.

KEY WORDS: 5,4′-didemethyltangeretin; cancer stem-like cells; epigenetics; p21; prostate cancer.

INTRODUCTION

Prostate cancer is the second most commonly diagnosed cancer and the fifth leading cause of cancer death in men worldwide. There are no obvious signs and symptoms in the early stage of prostate cancer, but as prostate cancer progresses to the late stages, the tumor presses the bladder and the ureter, resulting in frequent urination, hematuria, difficulty in micturition, or pain during urination (1). A healthy diet and regular physical activity play an important role to reduce the risk of prostate cancer (2). Prostate cancer cells can usually be removed by different treatment approaches; however, prostate cancer may recur due to the presence of cancer stem cells (3). Cancer stem cells are derived from the malignant transformation of differentiated cells and have the ability of self-renewal in the tumor tissues, thereby maintaining tumor differentiation, growth, and metastasis (4).

Epigenetic mechanisms can regulate gene expression without altering DNA sequence, resulting in a phenotypic change. The major epigenetic mechanisms include DNA methylation and histone modification (5). DNA methylation is regulated by DNA methyltransferases, mainly DNMTs 1, 3A, and 3B (6). Methylation of cytosine in the cytosine-phosphate-guanine (CpG) site is one of the most common modifications resulting in the inhibition of some gene expression, especially the tumor suppressor genes (7). Methyl-DNA–binding proteins (MBDs) binding to methylated CpG interferes with the interaction of the transcription factors with DNA, resulting in gene silencing (7). Chromatin remodeling is another important process-regulating gene expression. Nucleosome, the basic unit of chromatin, consists of DNA and histone. Histone modification can alter the tight

Guor-Jien Wei and Yen-Hsiang Chao contributed equally to this work.

Guest Editors: Ah-Ng Tony Kong and Chi Chen

[1] Institute of Food Safety and Health Risk Assessment, National Yang-Ming University, Taipei, Taiwan.
[2] Department of Bioscience Technology, Chung Yuan Christian University, Taoyuan City, Taiwan.
[3] Institute of Food Science and Technology, National Taiwan University, Taipei, Taiwan.
[4] Department of Pharmacology, School of Medicine, Tzu Chi University, Hualien City, Taiwan.
[5] To whom correspondence should be addressed. (e–mail: zysu@cycu.edu.tw)

and loose structure of the chromatin, resulting in transcriptional activation or repression, respectively (8). Some amino acids in the terminal peptide of histone may undergo post-translational modification, such as lysine acetylation (9). These dynamic histone modifications are catalyzed by some histone modifying enzymes, such as histone deacetylases (HDACs) (10).

Many phytochemicals available in vegetables and fruits have been shown to inhibit the development of prostate cancer by different mechanisms, such as apoptosis and cell cycle arrest (11). In recent years, studies have found that some phytochemicals may induce epigenetic modifications, including DNA methylation and histone modification to activate genes that are important for the prevention and treatment of human diseases (5). For example, astaxanthin in edible algae can reduce the level of methylated promoter and increase the expression of glutathione *S*-transferases (GSTs) in human prostate cancer LNCaP cells (12). It can also reduce the protein expression of DNMT 3B significantly and inhibits the activity of DNMTs and HDACs *in vitro* (13). The induction of tumor suppressor genes Cip1/p21 and $p16^{INK4a}$ by epigallocatechin-3-gallate (EGCG) through epigenetic regulation also plays a critical role in preventing cancer (14). In addition, some recent studies have been conducted in prostate cancer stem-like cells (CSLCs). High clonogenic prostate CSLCs with specific surface antigens $CD44^+/\alpha2\beta1hi/CD133^+$ can be isolated from human primary prostate cancer tissues (15,16). EGCG alone or in combination with quercetin and catechin can inhibit $CD44^+/CD133^+$ and, thus, can inhibit the growth and invasion of prostate cancer stem cells (17).

Citrus is a common fruit containing many nutrients which are beneficial to the body. Flavonoids, especially polymethoxylated flavones (PMFs), are the secondary metabolites present in citrus fruits having a wide range of pharmacological effects, including anti-cancer activity (18). PMF-enriched citrus peel extracts can induce apoptosis in various human breast cancer cells, and nobiletin (3′,4′,5,6,7,8-hexamethoxyflavone) is one of the main active PMFs (19). Nobiletin also inhibits the growth of prostate cancer PC-3 and DU145 cells via the Akt pathway (20,21). Tangeretin (4′,5,6,7,8-pentamethoxyflavone, PMF1) can induce G1 phase arrest or apoptosis in various human breast and colon cancer cells (22,23). Other PMF derivatives, such as 5-hydroxy-3,6,7,8,3′,4′-hexamethoxyflavone and 5-hydroxy-3,7,8,3′,4′-pentamethoxyflavone exhibit anticancer activities and induce G0/G1 phase arrest and increase the level of sub-G0/G1 phase in human lung cancer H1299 cells (24). 5-Hydroxy-6,7,8,3′,4′-pentamethoxyflavone (5-demethylnobiletin) and 5-hydroxy-3,6,7,8,3′,4′-hexamethoxyflavone cause apoptosis of human promyelocytic leukemia HL-60 cells (25).

Additionally, the anticancer potential of 5,4′-dihydroxy-6,7,8-trimethoxyflavone (5,4′-didemethyltangeretin, PMF2), a major colonic metabolite of 5-demethyltangeretin, has also been studied against several human cancer cell lines (26,27). However, the inhibitive effect and mechanism of PMF2 on human prostate cancer have not previously been investigated. In this study, we evaluated the effects of PMF1 and synthetic PMF2 on the growth of human prostate cancer LNCaP cells, CSLCs isolated from LNCaP cells, and normal RWPE-1 cells. The inhibitory mechanism including epigenetic regulation of PMF2 in the LNCaP cells was further elucidated.

MATERIALS AND METHODS

Materials

Bacteriological agar, Basal Medium Eagle (BME), dimethyl sulfoxide (DMSO), dithiothreitol (DTT), Nonidet P-40 (NP-40), phenylmethylsulfonyl fluoride (PMSF), propidium iodide, RNase A, sodium bicarbonate, and Triton X-100 were supplied by Sigma-Aldrich (St. Louis, MO, USA). DMEM/F12 medium, fetal bovine serum (FBS), gentamicin, glutamine, penicillin-streptomycin, RPMI-1640 medium, and trypsin-ethylenediaminetetraacetic acid (EDTA) were obtained from Gibco (Grand Island, NY, USA). Caspase-3, PARP, Bcl-2, Bad, Bax, HDAC 1, HDAC 2, HDAC 4/5/9, DNMT 1, DNMT 3A, DNMT 3B, and β-actin antibodies were obtained from GeneTex (Irvine, CA, USA). DNMT 2 antibody was obtained from Santa Cruz Biotechnology (Dallas, TX, USA). DNA methyltransferase M.SssI and restriction enzyme BstUI were obtained from New England Biolabs (Ipswich, MA, USA).

Synthesis of 5,4′-Didemethyltangeretin (PMF2)

The synthesis of PMF2 was performed according to the method described for the synthesis of 5,4′-didemethylnobiletin (28), except 4-benzyloxy-benzaldehyde was used instead of 4-benzyloxy-3-methoxy-benzaldehyde. The chemical structures of tangeretin (PMF1) and 5,4′-dihydroxy-6,7,8-trimethoxyflavone (PMF2) are shown in Fig. 1.

Cell Culture and Cell Viability Assay

Human prostate cancer LNCaP and normal prostate RWPE-1 cell lines were separately cultured in RPMI-1640 medium-containing 10% FBS at 37 °C in a humidified incubator in the presence of 5% CO_2. During treatment of the LNCaP and RWPE-1 cells, the new medium-containing 1% FBS were used after the cells were cultured in a medium-containing 10% FBS for 24 h. When performing cell viability assay, LNCaP or RWPE-1 cells at a density of 1.0×10^4 cells/100 μL were seeded in a 96-well plate. After 24 h, the cells were treated with various concentrations of PMF1 or PMF2 for 48 h. The cell viability was estimated using a CellTiter 96 aqueous one solution cell proliferation assay kit (Promega, Madison, WI) as described previously. The absorbance (ABS) was measured at a wavelength of 490 nm in a microplate spectrophotometer (Beckman, Brea, CA). Growth inhibition of 50% (GI_{50}) is the concentration of a compound which reduces the cell viability of treated cells by 50% with reference to untreated cells. The concentration at which the curve passes through the 50% of cell viability was calculated for the GI_{50} when the cells treated with various concentrations of compounds.

Isolation of the CSLCs

With slight modifications in the previously described method (29), prostate cancer CSLCs cells at a density of 1.0×10^4 cells were cultured on a 6-cm ultra-low culture dish

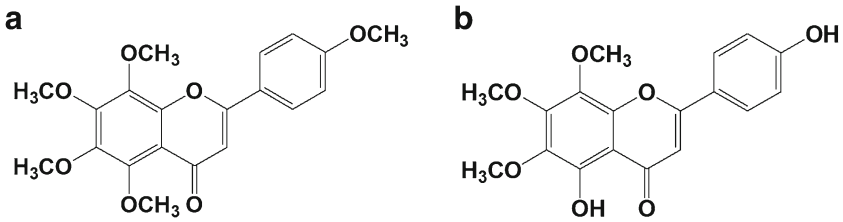

Fig. 1. Chemical structures of **a** tangeretin (PMF1) and **b** 5,4′-didemethyltangeretin (PMF2)

(Corning, Corning, NY) with 4.0 mL serum-free DMEM/F12 medium containing 20 ng/mL epidermal growth factor, 5 μg/mL insulin, 0.4% bovine serum albumin, and 2% B27. After 14 days of culture, the growing CSLCs were collected for the determination of CD166 mRNA expression and anchorage-independent growth.

Anchorage-Independent Growth Assay

Anchorage-independent growth assay was performed following a previously described method with some modifications (30). LNCaP cells and LNCaP CSLCs at a density of 8.0×10^3 cells were cultured in 1.0 mL of BME containing 0.33% bacteriological agar over 3.0 mL of BME-containing 0.5% bacteriological agar in 6-well plates. The cells were incubated with various concentrations of PMF2 at 37 °C in a humidified incubator in the presence of 5% CO_2 for 21 days. ImageJ software (version 1.80, National Institutes of Health (NIH)) was further used to measure and count the number of the colonies.

Cell Cycle and Sub-G1 Phase Analysis

According to the method in the previous study (31), LNCaP cells were seeded in a 10-cm dish at a density of 1×10^6 cells/dish for 24 h. The medium was replaced with new medium containing different concentrations of PMF2. After 48 h, the cells were washed and collected in 3.0 mL ice-cold 70% alcoholic solution. The cell cycle analysis was performed with propidium iodide stain as described previously. Briefly, 70% alcoholic solution was discarded after centrifugation, and the cells were suspended in propidium iodide stain solution-containing 4 μg/mL propidium iodide, 0.1 mg/mL RNase A, and 0.1% Triton X-100 in a dark room for 30 min. The stained cells were analyzed by a flow cytometer (Thermo Fisher Scientific, Waltham, MT).

Western Blot

The cells treated with or without PMF2 were harvested and suspended in radioimmunoprecipitation assay (RIPA) buffer (Cell Signaling Technology, Danvers, MA). Following that, the total protein concentration of the lysate was determined by bicinchoninic acid (BCA) protein assay (G-Bioscience, St. Louis, MO). The specific protein expression was analyzed by Western blot. Briefly, the lysate (25 μg) was mixed with sodium dodecyl sulfate (SDS)-loading dye. The protein was denatured at 95 °C for 5 min and then subjected to SDS-polyacrylamide gel electrophoresis (SDS-PAGE). The separated proteins were subsequently transferred onto a polyvinylidene difluoride (PVDF) membrane using a semidry transfer system (Bio-Rad, Hercules, CA). After transfer, the PVDF membrane was washed with Tris-buffered saline-containing 0.1% Tween 20 (TBST) and then blocked with TBST containing 3% skim milk. The proteins on the PVDF membrane were hybridized with specific primary antibodies. Horseradish peroxidase (HRP)-conjugated secondary antibodies and Immobilon western chemiluminescent HRP substrate (Millipore, Burlington, MA) were used to detect the immunoblots. The images were captured by Luminescent Image Analyzer (Fujifilm, Tokyo, Japan). ImageJ densitometry software (version 1.80, NIH) was further used to quantify the intensity of bands.

RNA Isolation and Quantitative Real Time-Polymerase Chain Reaction (qRT-PCR)

According to the manufacturer's instructions (GeneDireX, Las Vegas City, NV), the total RNA in the harvested cells was extracted using a total RNA isolation kit, and then their first-strand cDNA was synthesized using a GScript first-strand synthesis kit. The first-strand cDNA was further mixed with specific primers and Power SYBR Green PCR Master Mix (Bio-Rad, Hercules, CA). The relative RNA expression was analyzed using Connect™ Real Time PCR Detection System (Bio-Rad, Hercules, CA). The following primers were used: GAPDH (sense 5′-TCG ACA GTC AGC CGC ATC TTC TTT-3′ and antisense 5′- ACC AAA TCC GTT GAC TCC GAC CTT-3′) (32), p21 (sense 5′- TGA CCC TGA AGT GAG CAC AGC C-3′ and antisense 5′- GCC GAG AGA AAA CAG TCC AGG C-3′) (33), and CD166 (sense 5′-TAG CAG GAA TGC AAC TGT G-3′ and antisense 5′-CGC AGA CAT AGT TTC CAG CA-3′).

In Vitro Methylation Assay

This assay was adapted from the previous study with slight modifications (34). The genomic DNA was extracted from the LNCaP cells using genomic DNA isolation kit (GeneDireX, Las Vegas City, NV). The $p16^{INK4a}$ DNA fragment (−422/+401) was amplified by PCR using ZymoBIOMICS™ PCR premix (Zymo Research, Irvine, CA) according to the manufacturer's instructions. The primers for amplifying the $p16^{INK4a}$ DNA fragment were as follows: sense 5′-GGC TCC TCC GCA TTC TC-3′ and antisense 5′-CTC GTC GAA AGT CTT CCA TTC T-3′. The PCR product as a substrate was further recovered using PCR cleanup and gel extraction kit (GeneDireX, Las Vegas City, NV). DNA substrate (200 ng), SAM (*S*-adenosyl methionine, 160 μM), and M.SssI (CpG methyltransferase, 0.1 units) were mixed with 20 μL of 1X NEB buffer containing-different concentration of PMF1 or PMF2 at 37 °C for 1 h. Subsequently, 1.0 μL of a restriction enzyme BstUI (10 units/μL)

was added to each reaction at 60 °C for another 1 h to digest the unmethylated DNA fragments. The DNA products were separated in 2% agarose electrophoresis with Novel Juice (GeneDireX, Las Vegas City, NV) and documented using a UV gel system (Vilber, Charles, France). The intensity of bands by densitometry was further quantified by ImageJ software (version 1.80, NIH).

Bisulfite Conversion and Methylation Specific PCR

The genomic DNA was extracted from the LNCaP cells treated with various concentrations of PMF2 using a genomic DNA isolation kit (GeneDireX, Las Vegas City, NV) following the manufacturer's instructions. DNA was subjected to bisulfite conversion using an EZ DNA methylation-lightning kit (Zymo Research, Irvine, CA) which converted cytosine without methyl group to uracil. Before the Methylation Specific PCR (MSP) assay, the amount of bisulfite converted to p21 DNA fragment was determined using PCR, and the primers used were as follows: sense 5′-GTG AGT TAG AAA GGG GGT TTA TTT T-3′ and antisense 5′-CTC TCT CAC CTC CTC TAA ATA CCT C-3′ (35). The same amount of the converted p21 DNA fragment from each treatment was further used for the MSP assay, and the primers used were as follows: methylated-sense 5′-TAC GCG AGG TTT CGG GATC-3′, methylated-antisense 5′-CCC TAA TAT ACA ACC GCC CCG-3′, unmethylated-sense 5′-GGA TTG GTT GGT TTG TTG GAA TTT-3′, and unmethylated-antisense 5′-ACA ACC CTA ATA TAC AAC CAC CCC A-3′ (35). The methylated and unmethylated p21 fragments were amplified using ZymoTaq™ PreMix kit (Zymo Research, Irvine, CA) with the following PCR conditions: initial denaturation at 95 °C for 10 min, 40 cycles of 95 °C for 45 s, 50 °C for 30 s, and 72 °C for 45 s followed by a final extension at 72 °C for 7 min. The concentration of the PCR products was analyzed in 2% agarose electrophoresis with Novel Juice (GeneDireX, Las Vegas City, NV) and documented using a UV gel system (Vilber, Charles, France). ImageJ densitometry software (version 1.80, NIH) was used for quantifying the intensity of bands.

Interaction between PMF2 and DNMTs

The *ex vivo* binding assay was performed to study the interaction between PMF2 and DNMTs using CNBr-activated Sepharose 4B beads (GE Healthcare, Pittsburgh, PA) following a previously described method with slight modifications (36). Briefly, beads were washed with HCl (1.0 mM) and then with a coupling buffer (containing 0.1 M $NaHCO_3$ and 0.5 M NaCl, pH 8.3) for 3 times. PMF2 was mixed with the beads in the coupling buffer at 4 °C and kept overnight. After removing the supernatant, the PMF2-bound beads were washed with Tris-HCl buffer (pH 8.0) at 4 °C overnight. The PMF2 bound beads were then washed with acetate buffer (0.1 M, containing 0.5 M NaCl, pH 4.0), followed by Tris-HCl buffer (0.1 M, containing 0.5 M NaCl, pH 8.0). The washing with alternating buffer and Tris-HCl buffer was repeated 4 times. Finally, the PMF2 bound beads were maintained in an equal amount of sterilized PBS and stored at 4 °C. LNCaP cell lysate was prepared with a lysis buffer (pH 7.5)-containing 50 mM Tris-HCl, 5 mM EDTA, 150 mM NaCl, 1 mM DTT, 0.5% NP-40, 0.2 mM PMSF, and 1X protease inhibitor cocktail. Beads or PMF2 bound beads and lysate protein were mixed in 50 mM Tris-HCl buffer (pH 7.5, containing 5.0 mM EDTA, 150 mM NaCl, 1 mM DTT, and 0.01% NP-40, and 2 μg/mL BSA) at 4 °C overnight, followed by 50 mM Tris-HCl washing buffer (pH 7.5, containing 5.0 mM EDTA, 150 mM NaCl, 1.0 mM DTT, 0.01% NP-40, and 0.02 mM PMSF). The supernatant was removed, and the pellet was denatured with a loading dye at 95 °C for 5 min. After centrifugation, the supernatant was subjected to SDS-PAGE and Western blot.

Computer-Simulated Binding to DNMT

The peptide sequence of the catalytic domain of human DNMT 2 is very similar to that of the other DNMTs, including DNMTs 1, 3A, and 3B (37). Referring to previous studies, the binding mode of PMF2 and human DNMT 2 catalytic domain was predicted using DockingServer (https://www.dockingserver.com) (38). The three-dimensional chemical structures of PMF2 and SAM were confirmed using Jmol (http://www.jmol.org). The information of DNMT 2 structure was obtained from the database of RCSB Protein Data Bank (https://www.rcsb.org/structure/1g55).

Statistical Analysis

The experimental results are represented as the mean ± standard deviation (SD). One-way ANOVA with Duncan's new multiple range test was performed to compare the differences among the treatment groups. Student's paired *t* test was performed to compare the significant differences between the treatment and control groups. Some analyses were performed using SAS software (version 9.4, SAS Institute Inc., Cary, NC, USA). A p value of < 0.05 was considered as statistically significant.

RESULTS

PMF2-Induced Apoptosis in Human Prostate Cancer LNCaP Cells

We have evaluated the inhibitory effects of PMF1 and its derivative PMF2 on the growth of human prostate cancer LNCaP cells. As shown in Fig. 2a, both PMF1 (10–20 μM) and PMF2 (5–20 μM) significantly reduced the viability of LNCaP cells after treatment for 48 h ($p < 0.05$). We also found that PMF2 (GI_{50} 14.6 μM) more effectively inhibited the growth of LNCaP cells as compared with PMF1 ($GI_{50} > 20$ μM). On the other hand, we treated human prostate normal RWPE-1 cells with PMF1 and PMF2 for 48 h to evaluate their cytotoxic activities against the normal prostate RWPE-1 cells (Fig. 2b). We found that PMF1 (5–20 μM) did not affect the growth of RWPE-1 cells. As compared with LNCaP cells, PMF2 caused less cytotoxicity to the RWPE-1 cells ($GI_{50} > 20$ μM).

In order to elucidate the mechanism of the inhibitory effects of PMF2 on LNCaP cells, propidium iodide-staining followed by flow cytometry was performed. As shown in Fig. 2c, PMF2 at a

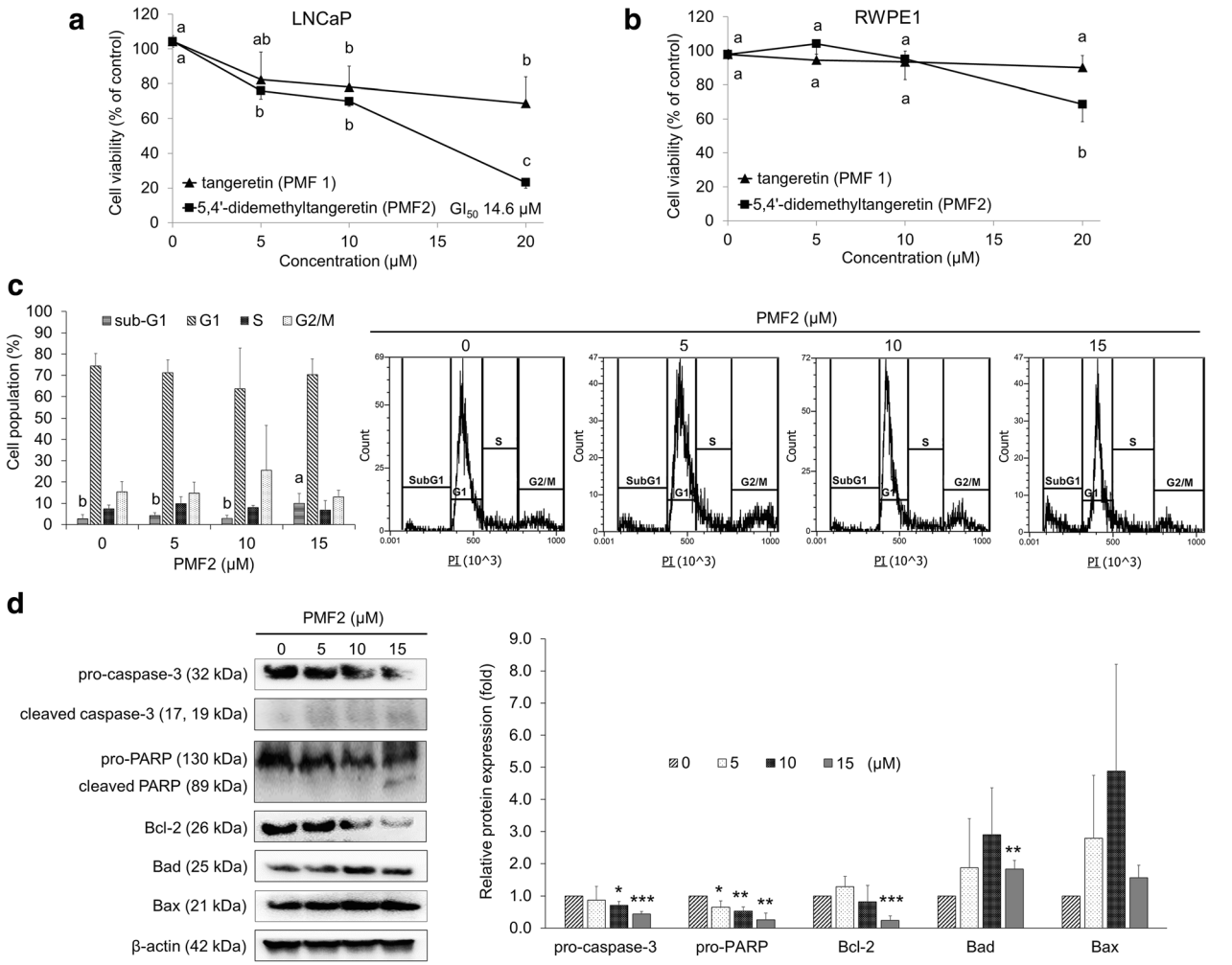

Fig. 2. Effects of PMF1 and PMF2 on the growth of human prostate cancer LNCaP and normal RWPE-1 cells. (**a**, **b**) LNCaP and RWPE-1 cells at 1.0×10^4 cells/well density were seeded in a 96-well plate for 24 h, respectively. The cells were then incubated with different concentrations of PMF1 or PMF2 for another 48 h. The cell viability was determined by MTS assay. The data are represented as the mean ± SD ($n = 3$). Significant differences among the groups treated with the same compounds are indicated with different letters ($p < 0.05$). (**c**) LNCaP cells at 1.0×10^6 cells/dish density were seeded in a 10-cm dish for 24 h and then incubated with different concentrations of PMF2 for another 48 h. DNA in the cells was stained by propidium iodide (PI) and analyzed using flow cytometry. The data are represented as the mean ± SD ($n = 3$). Significant differences among the groups are indicated with different letters ($p < 0.05$). (**d**) Protein expression was determined by Western blot, and β-actin was used to normalize the protein expression. The data are represented as the mean ± SD ($n = 3$). Significant differences in the treatment group as compared with the untreated control group are marked ($^{*}p < 0.05$, $^{**}p < 0.01$, $^{***}p < 0.001$)

concentration of 15 μM significantly increased the population of LNCaP cells in the sub-G1 phase after 48 h of treatment ($p < 0.05$). It suggested that PMF2 might induce apoptosis in the LNCaP cells. Furthermore, we determined the expression of apoptosis-related proteins in the LNCaP cells after treatment with different concentrations of PMF2 for 48 h (Fig. 2d). The results showed that PMF2 at 10 and 15 μM concentrations significantly decreased the levels of procaspase-3 ($p < 0.05$), while the levels of cleaved caspase-3 were increased in a dose-dependent manner, suggesting that PMF2 may activate caspase-3. The protein expression of pro-poly ADP-ribose polymerase (pro-PARP) was significantly decreased by PMF2 (5–15 μM) ($p < 0.05$). In addition, PMF2 at 15 μM concentration significantly decreased the level of the anti-apoptotic protein Bcl-2 ($p < 0.001$) and increased the level of the proapoptotic protein Bad ($p < 0.01$). PMF2 also increased the expression of the proapoptotic protein Bax slightly. These results indicated that PMF2-induced apoptosis in the LNCaP cells.

PMF2 Inhibited the Anchorage-Independent Growth in the LNCaP Cells

Furthermore, we performed soft agar colony formation assay to evaluate the inhibitory efficacy of PMF2 on LNCaP cells after 14 days of treatment (Fig. 3). PMF2 at a concentration of 15 μM significantly (around 70%) suppressed anchorage-independent growth of the LNCaP cells. These results suggested that the anticancer activities of PMF2 were stronger than that of PMF1.

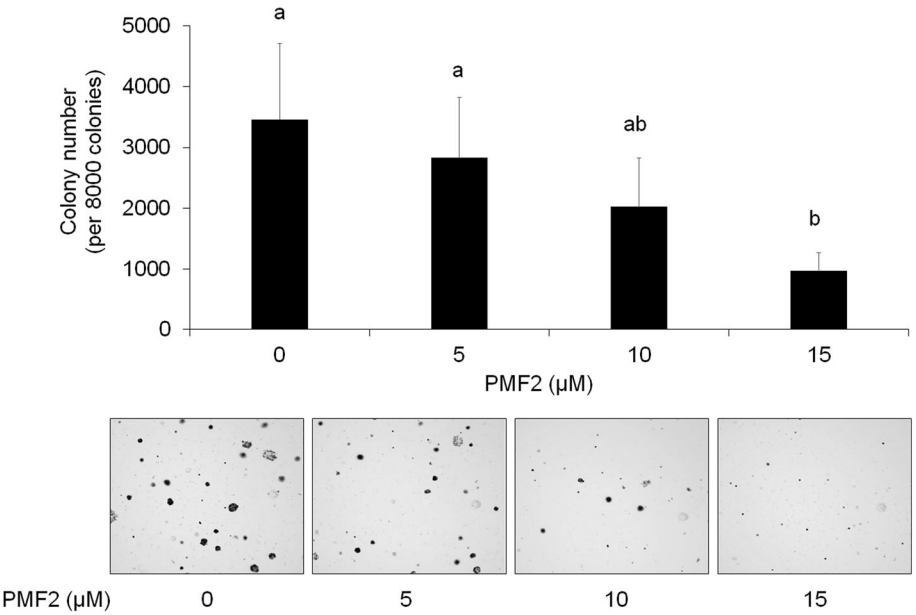

Fig. 3. Effects of PMF2 on the anchorage-independent growth of human prostate cancer LNCaP cells. LNCaP cells (8000 cells/well) were seeded in a 6-well plate in soft agar containing different concentrations of PMF2 for 14 days. The number of colonies was observed under a microscope. The data are represented as the mean ± SD ($n = 3$). Significant differences among the groups treated with the same compounds are indicated with different letters ($p < 0.05$)

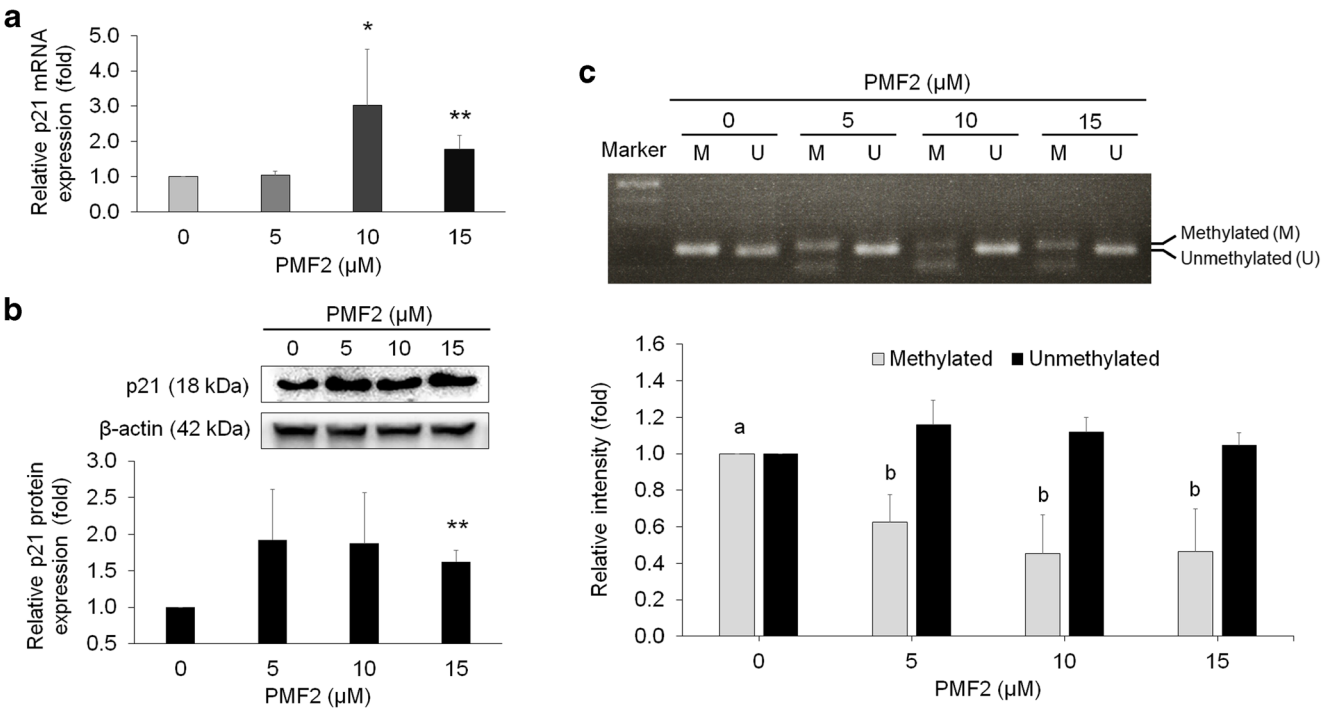

Fig. 4. Effects of PMF2 on the levels of tumor suppressor gene p21 in human prostate cancer LNCaP cells. (**a**) LNCaP cells at 1.0×10^6 cells/dish density were seeded in a 10-cm dish for 24 h and then incubated with different concentrations of PMF2 for another 48 h. The expression of p21 mRNA was determined using qPCR, and GAPDH was used for normalization. (**b**) The expression of p21 protein was determined using Western blot, and β-actin was used for normalization. The data of p21 mRNA and protein expressions are represented as the mean ± SD ($n = 4$ and $n = 3$, respectively). Significant differences in the treatment group as compared to the untreated control group are marked ($^{*}p < 0.05$, $^{**}p < 0.01$). (**c**) The genomic DNA was extracted from the cells and then treated with sodium bisulfite. The bisulfite-treated DNA was amplified by PCR using 2 primer pairs that separately targeted the methylated (M) and unmethylated (U) regions. The data are represented as the mean ± SD ($n = 3$). Significant differences among the groups are indicated with different letters ($p < 0.05$)

PMF2 Increased mRNA and Protein Expression of p21 by Suppressing Promoter Methylation in the LNCaP Cells

The mRNA and protein levels of tumor suppressor gene p21 in the LNCaP cells were further estimated after treatment with PMF2 for 48 h. As shown in Fig. 4a, PMF2 at 10 and 15 μM concentrations significantly induced the mRNA expression of p21 ($p < 0.05$ and 0.01, respectively). Similarly, PMF2 at 15 μM concentration also increased the protein expression of p21 significantly ($p < 0.01$, Fig. 4b). In order to ensure whether PMF2 restored p21 mRNA expression through epigenetic modifications in the LNCaP cells, we further analyzed the levels of methylated and unmethylated p21 promoter using MSP assay after bisulfite conversion. The results showed that PMF2 (5–15 μM) significantly reduced the level of methylated p21 promoter ($p < 0.05$, Fig. 4c). Therefore, PMF2 might trigger the expression of the p21 gene by demethylation of the p21 promoter region.

PMF2 Regulated the Levels of Epigenetic Modifying Enzymes in the LNCaP Cells and Blocked *In Vitro* DNA Methyltransferase Activity

After 48 h of pretreatment of the LNCaP cells with different concentrations of PMF2, the levels of histone deacetylases (HDACs 1, 2, and 4/5/9), and DNA methyltransferases (DNMTs 1 and 3B) were determined (Fig. 5a). We found that PMF2 at 10 and 15 μM concentrations significantly suppressed the expression of HDACs 1 and 4/5/9 ($p < 0.05$). PMF2 at a concentration of 15 μM also significantly reduced the levels of HDAC 2 and DNMT 3B, although PMF2 slightly reduced DNMT 1 expression. Furthermore, we compared the inhibitory effects of PMFs (0–500 μM) on recombinant DNA methyltransferase M.SssI activity. A substrate DNA amplified from the CpG-enriched $p16^{INK4a}$ DNA fragment (−422/+401) in the LNCaP cells were used (Fig. 4b, c). We observed that

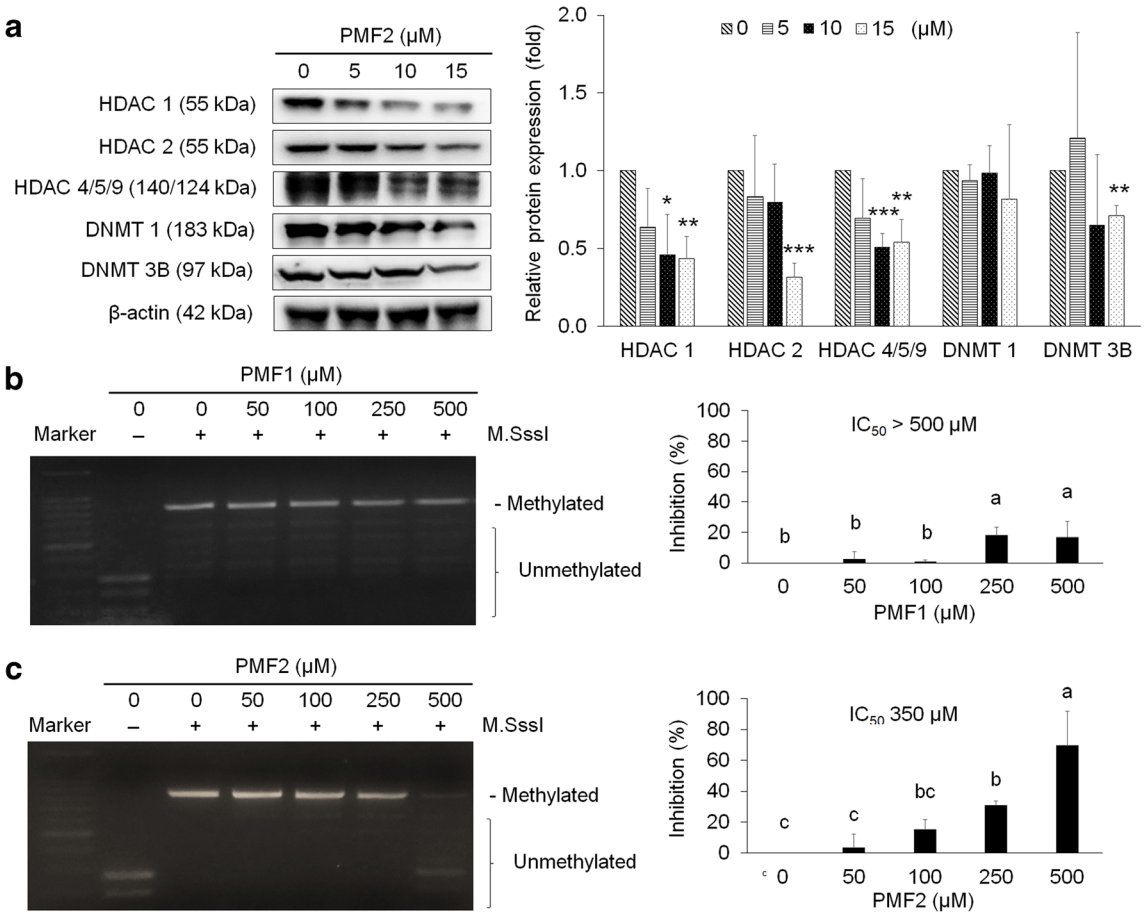

Fig. 5. Effects of PMF2 on protein expression of epigenetics modifying enzymes in human prostate cancer LNCaP cells and *in vitro* DNA methyltransferase (M.SssI) activity. (**a**) LNCaP cells at 1.0×10^6 cells/dish density were seeded in a 10-cm dish for 24 h and then incubated with different concentrations of PMF2 for another 48 h. The protein expression was determined using Western blot, and β-actin was used for normalization. Significant differences in the treatment group as compared with the untreated control group are marked ($^{*}p < 0.05$, $^{**}p < 0.01$, $^{***}p < 0.001$). (**b**, **c**) The PCR product of $p16^{INK4a}$ gene fragment (−422/+401) was incubated with M.SssI, a recombinant DNMT, and different concentrations of PMF2 at 37 °C for 1 h. A restriction enzyme BstUI was added and then incubated for another 1 h at 60 °C. The digested products were separated in 2% agarose gel and then documented. The inhibitory activities of PMF2 were calculated from the intensity of methylated fragments and compared with the untreated control group. The data are represented as the mean ± SD ($n = 3$). Significant differences among the groups are indicated with different letters ($p < 0.05$)

both PMF1 and PMF2 at 250 and 500 μM concentrations significantly suppressed M.SssI activity as compared with the control group ($p < 0.05$). Based on the GI_{50} data, we further found that PMF2 exhibited stronger inhibitory effects than PMF1. These results indicated that PMF2 might downregulate some epigenetic modifying enzymes and block DNA methyltransferase activity, resulting in the re-expression of tumor-suppressing gene p21 in the LNCaP cells.

Interaction between PMF2 and DNMTs

It is speculated that PMF2 may interact with intracellular DNMTs and affect their activities. Therefore, a pull-down assay was performed using Sepharose 4B-PMF2 beads to explore whether PMF1 interacts with DNMTs in the LNCaP cell lysate. The results showed that DNMTs 1, 2, and 3A in the cell lysates can be detected after incubation with PMF2-Sepharose 4B beads, but not with blank Sepharose 4B-beads, suggesting that DNMTs 1, 2, and 3A can bind to PMF2 (Fig. 6a–c). Because of the highly conserved catalytic domain in these DNMTs (37), the structure of DNMT 2 catalytic domain was selected for the simulated binding of PMF2 and *S*-adenosyl methionine (SAM). As shown in Fig. 6d, PMF2 and SAM had interactions with the catalytic regions of DNMT 2. It indicated that there were several interactions between PMF2 and DNMT 2, including a polar (hydrogen at 4′ position and asparagine 139) and hydrophobic (ring B and proline 107, and rings A and C, and leucine 112) interactions. In addition, the free energy for binding of PMF2 and SAM with DNMT 2 were found to be −3.98 and −4.53 kcal/mol, respectively. The inhibition constant (Ki) for the binding of PMF2 and SAM with DNMT 2 were 1.21 and 0.48 mM, respectively. These results implied that PMF2 might be a strong competitor of SAM for binding to the catalytic regions of DNMTs, and it interferes with the activity of DNMTs to catalyze DNA methylation.

PMF2 Suppressed the Growth of Isolated LNCaP CSLCs

The LNCaP cells were cultured in ultra-low-attachment culture dishes with serum-free medium. The morphology of

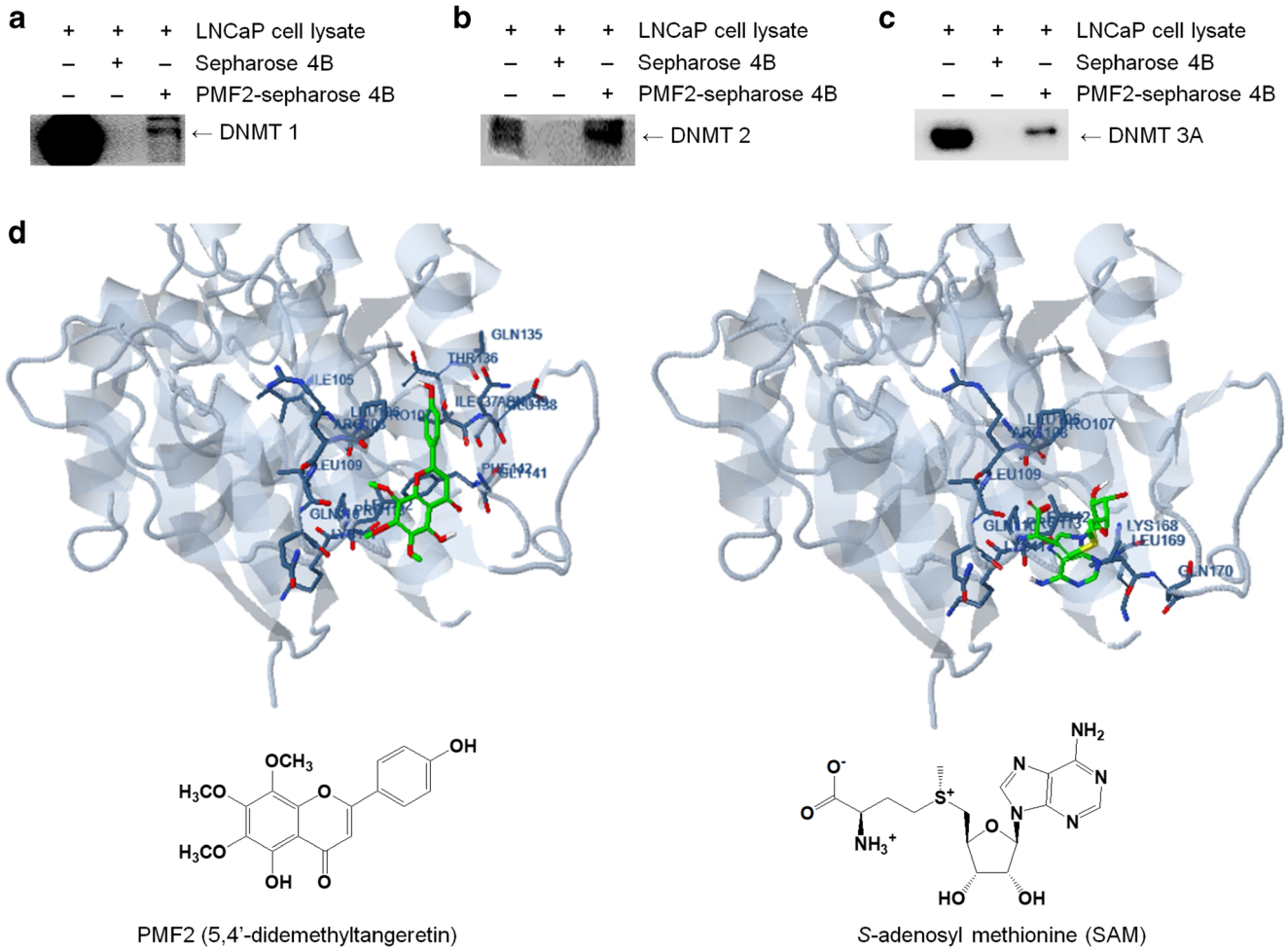

Fig. 6. Interaction between PMF2 and DNMTs in human prostate cancer LNCaP cells. (**a**–**c**) The prepared cell lysate was precipitated with Sepharose 4B or PMF2-Sepharose 4B beads. The protein expression in DNMTs 1, 2, and 3A was determined by Western blot. The data are representative of 3 separate experiments eliciting similar results. (**d**) Computational docking model of PMF2 and DNMT 2. The interaction between PMF2 and C-terminal catalytic domain of DNMT 2 in the molecular modeling is shown. The C-terminal catalytic domain of human DNMT 2 (PDB: 1G55) obtained from Protein Data Bank was selected to perform the predicted docking model with PMF2 and *S*-adenosyl methionine using DockingServer (https://www.dockingserver.com/web)

the spheres was observed after 0–14 days, and we found that the spheres grew fast from 4 to 7 days (Fig. 7a). In order to confirm whether the cells separated from the LNCaP parental cells had characteristics of cancer stem cells, we used qRT-PCR to detect CD166 mRNA expression in the spheres after 14 days. The results showed that the isolated spheres had a significantly higher level (approximately 1.5-fold) of CD166 mRNA as compared to the parental cells ($p < 0.01$, Fig. 7b), advocating that the spheres might be CSLCs. We further performed a colony formation assay in soft agar to evaluate the inhibitory effects of PMF2 on anchorage-independent growth of the LNCaP CSLCs for 21 days, and it showed that PMF2 at 15 μM concentration exhibited significant suppressive effects as compared with the control group ($p < 0.05$, Fig. 7b). These results suggested that PMF2 might have a potential to inhibit the growth of the prostate cancer stem cells.

DISCUSSION

Many studies have demonstrated that various citrus PMFs exhibit anticancer effects in different cancer cells, such as tangeretin (4′,5,6,7,8-pentamethoxyflavone, PMF1), 5-demethyltangeretin (5-hydroxy-4′,6,7,8-tetramethoxyflavone), naringin (4′,5,7-trihydroxyflavanone 7-rhamnoglucoside), hesperetin (3′,5,7-trihydroxy-4′-methoxyflavanone), and nobiletin (3′,4′,5,6,7,8-hexamethoxyflavone) (20,22,39,40). Among these compounds, PMF1 has an anticancer property which can induce cell cycle arrest in human breast cancer MCF-7 and MDA-MB-435 and colon cancer HT-29 cells (22). 5-Demethyltangeretin, a PMF1 derivative, shows stronger tumor-suppressive effects than tangeretin (39). It suggests that the hydroxyl group in the 5 positions of the ring A in PMF1 derivatives may play a critical role in determining the anticancer effects. In the beginning of this study, we have evaluated the anticancer effects of synthetic 5-demethyltangeretin in the LNCaP cells (data not shown). It is, however, difficult to evaluate the GI_{50} of 5-demethyltangeretin due to its low solubility in the medium. Another compound 5,4′-didemethyltangeretin (PMF2) which is a major colonic metabolite of 5-demethyltangeretin was also been synthesized in this study (26,28). Interestingly, PMF2 with better solubility exhibited much stronger inhibitory effects on human prostate cancer LNCaP cells than PMF1 (Fig. 2a). Furthermore, PMF2 at 15 μM concentration demonstrated a low

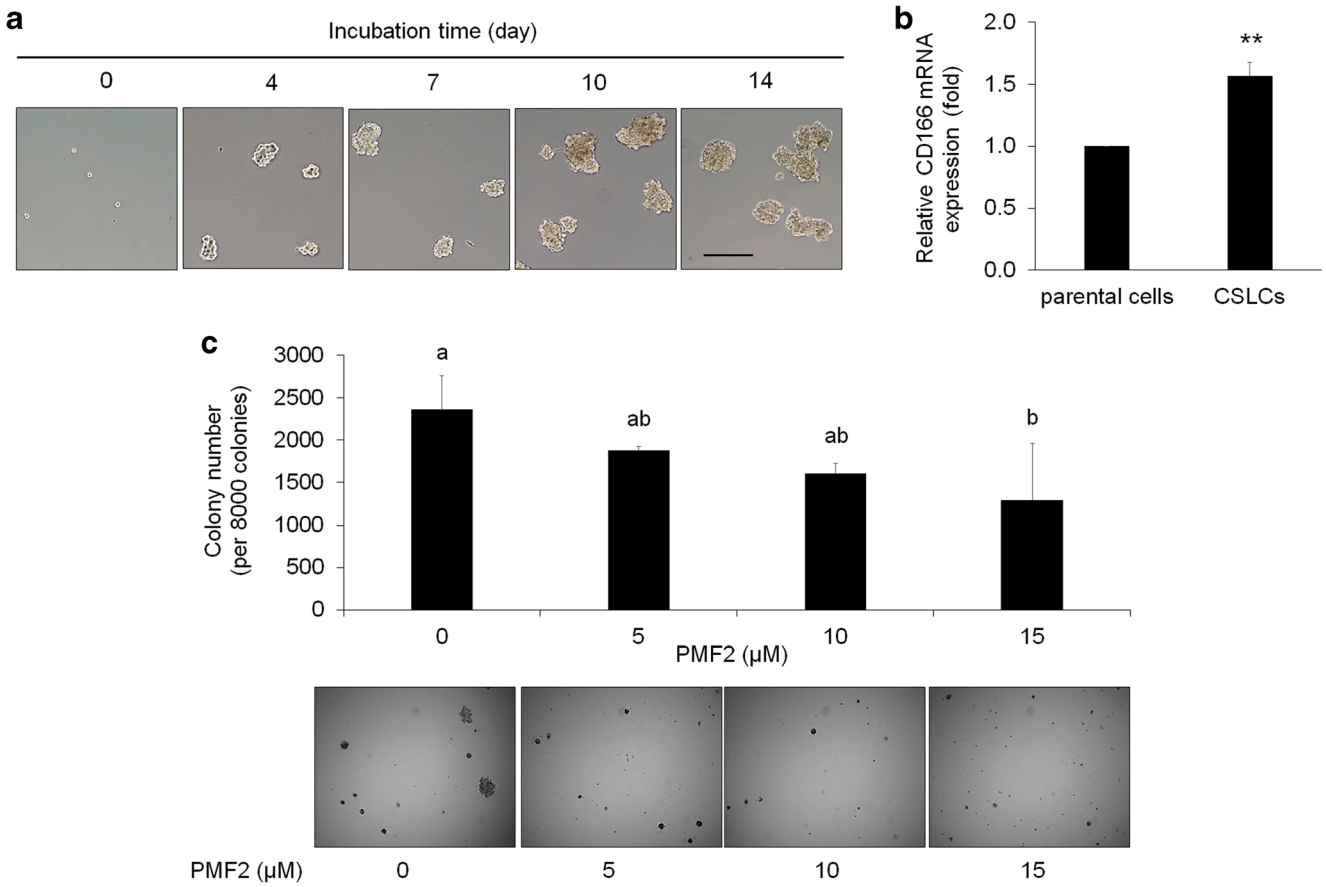

Fig. 7. Isolation and effects of PMF2 on anchorage-independent growth of LNCaP cancer stem-like cells (CSLCs). (**a**) LNCaP cells at 1.0×10^3 cells/dish density were cultured in a serum-free medium on 6 cm ultra-low attachment culture dishes for a fixed number of days. The morphology of the cells was observed under a microscope (× 100, "—" = 1 mm). (**b**) RNA from the stem cell biomarker CD166 gene present in LNCaP CSLCs after 14 days of culture was extracted using RNA isolation kit and mRNA levels of CD166 were determined using qPCR. mRNA expression of GAPDH was determined for normalization. The data are represented as the mean ± SD ($n = 3$). Significant differences in the CSLCs as compared with the parental cells are marked ($^{**}p < 0.01$). (**c**) LNCaP CSLCs at 8000 cells/well density were seeded in soft agar with different concentrations of PMF2 for 21 days in 6-well plates. The colonies were observed under a microscope. The data are represented as the mean ± SD ($n = 3$). Significant differences among the groups are indicated with different letters ($p < 0.05$)

cytotoxic potential against human prostate RWPE-1 cells while it effectively suppressed the anchorage-independent growth of the LNCaP cells (Figs. 2b and 3). This indicated that PMF2 can be a potential anticancer drug candidate.

Recently, the mechanisms of the anticancer activities of citrus PMFs have been studied. A citrus peel extract enriched with PMFs can significantly reduce tumor weight and expression of tumor metastasis-associated proteins including MMP-2 and MMP-9 in human prostate cancer PC-3 cells xenografted mice (18). Some PMFs, such as naringin and hesperetin can induce cell cycle arrest in the cancer cells (39,41). Nobiletin not only induces apoptosis in human breast cancer MCF-7 cells but also inhibits angiogenesis in human prostate cancer PC-3 and DU145 cells (20,40,42). 5-Hydroxy-7-methoxyflavone also induces apoptosis in human colon cancer HCT-116 cells by increasing the level of activated caspase-3, Bax, and BID, and decreasing the level of Bcl-2 (43). 5,3′-Dihydroxy-3,6,7,8,4′-pentamethoxyflavone significantly inhibits the growth of human blood cancer KBM-5 cells by upregulating the tumor suppressor gene p21 and downregulating the anti-apoptotic gene Bcl-2 (44). This is the first study to demonstrate that PMF2 induces apoptosis in the LNCaP cells through activating the caspase-3 pathway, upregulating Bad and Bax, and downregulating Bcl-2 (Fig. 2c, d). These results might correlate well with the PMF2-induced p21 re-expression (Fig. 4a, b). Accumulating evidence shows that p21-induced apoptosis plays an important role in anticancer activity of some phytochemicals, such as ursolic acid and sulforaphane (45,46). In this study, the level of methylation in the promoter region of the tumor suppressor gene p21 was also significantly reduced by PMF2 (Fig. 4c). Similar to PMf2, sulforaphane increases mRNA and protein expression of p21 and Bax in PC-3 cells through epigenetic regulation resulting in cell cycle arrest and apoptosis (47). However, it would be worthwhile to study if PMF2 might suppress the survival of prostate cancer through other pathways in the future.

Molecular docking models have predicted interactions of EGCG with DNMT 3B and HDAC 1, resulting in the inhibition of DNMT 3B and HDAC 1 activity by EGCG treatment in human cervical cancer HeLa cells (48). EGCG treatment also significantly suppressed promoter DNA methylation and enhanced mRNA expression of the tumor-suppressor genes, including retinoic acid receptor-β (RARβ), cadherin 1 (CDH1), and death-associated protein kinase-1 (DAPK1) in HeLa cells (48). The silenced Cip1/p21 and $p16^{INK4a}$ genes can be restored by EGCG reducing DNA methylation and increasing histone acetylation in human skin cancer A431 cells, contributing to the anti-skin cancer activity of EGCG (14). In this study, PMF2 suppressed the protein expression of epigenetic regulatory enzymes, including DNMTs 1 and 3B as well as HDACs 1, 2, and 4/5/9 (Fig. 5a). Furthermore, we also found that PMF2 has interactions with DNMTs 1, 2, and 3A (Fig. 6a–c). DNMT2 is the smallest molecular DNA methyltransferase in mammals and has the ability to methylate tRNA (49). The C-terminal catalytic domain of DNMT 2 shares strong sequence homology with the other DNMTs, including DNMTs 1, 3A, and 3B (37). This catalytic region in DNMTs predominantly binds to *S*-adenosyl methionine (SAM) and further transfers the methyl group

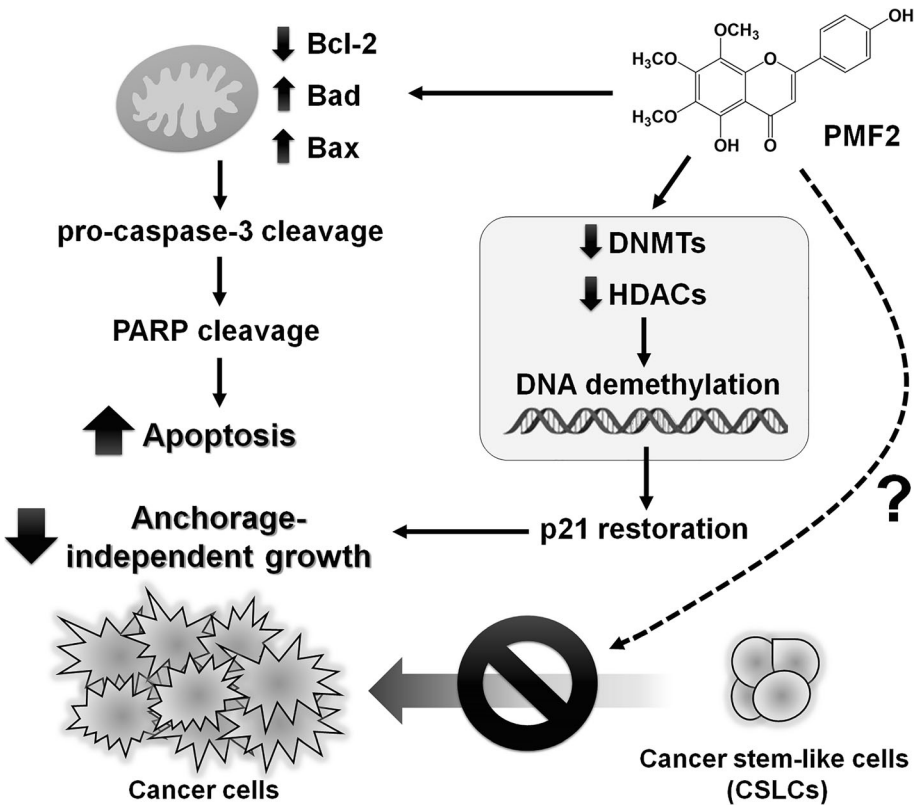

Fig. 8. Proposed mechanism of the anticancer activity of PMF2 against prostate cancer through induction of mitochondria-mediated apoptosis, epigenetic restoration of p21 gene, and growth inhibition of cancer stem cells

from SAM to DNA or tRNA (37). Therefore, we further developed a computer-simulated binding model between PMF2 and the catalytic domain of DNMT 2 (Fig. 6d). The results advocated that PMF2 strongly competes with SAM for binding to the catalytic position of DNMTs. Interestingly, we also observed that PMF2 effectively reduced the *in vitro* methylation in human $p16^{INK4a}$ DNA fragment (−422/+401) by inhibiting the activity of M.SssI, a DNA methyltransferase, and its inhibitory potential is greater than that of PMF1 (Fig. 5b, c). Taken together, PMF2 not only affects the activity of the enzymes through interactions with DNMTs but also reduces the protein expression of DNMTs and HDACs. Thus, PMF2 inhibits p21 promoter methylation and significantly increases p21 mRNA level and protein expression.

Additionally, cell surface CD166 has been identified as an important prognostic biomarker in the previous studies in many cancer stem cells (CSCs), including prostate cancer (50). CD166 also plays a critical role in metastasis and cancer recurrence after treatment (51). In the present study, we separated the spheroids from human prostate cancer LNCaP cell line in a serum-free medium using ultra-low attachment dishes (Fig. 7a). These spheroids were defined as CSLCs after growth for 14 days since they had a higher CD166 mRNA expression as compared with the parental cells (Fig. 7b). We further found that PMF2 treatment significantly suppressed the anchorage-independent growth of the LNCaP CSLCs (Fig. 7c), suggesting that PMF2 might inhibit metastasis and recurrence in prostate cancer.

CONCLUSION

In conclusion, 5,4′-didemethyltangeretin (PMF2), a synthetic tangeretin (PMF1) derivative, exhibited more potent anticancer properties against human prostate cancer LNCaP cells than PMF1. On the other hand, PMF2 had low cytotoxic effects against the normal prostate RWPE-1 cells. As shown in Fig. 8, PMF2-mediated apoptosis in the LNCaP cells might be triggered through downregulation of Bcl-2, upregulation of Bad and Bax, and activation of caspase-3 and PARP. We further found that PMF2 induced the transcriptional activation of p21 gene in the LNCaP cells by decreasing the levels of HDACs and DNMTs by blocking *in vitro* DNA methyltransferase activity and demethylating the promoter region of p21 gene. Based on the results of pull-down assay and computer docking models, PMF2 can be considered as a strong competitor of SAM to bind at the catalytic regions of DNMTs. This is the first study to show that a tangeretin derivate can inhibit the growth of human prostate cancer cells through epigenetic regulations and interaction with DNMTs. In addition to the anchorage-independent growth inhibition and apoptosis in the LNCaP cells, PMF2 can also inhibit the tumorigenesis of LNCaP CSLCs with high expression of CD166 isolated from the parental cells. The molecular mechanism, however, needs to be clearly elucidated in future studies.

FUNDING INFORMATION

This research is supported in part by institutional funds and by the MOST 105-2815-C-033-013-B and MOST 105-2320-B-033-001 from the Ministry of Science and Technology. We thank all the members of Dr. Su's lab for their helpful discussion of this work.

REFERENCES

1. Schaake W, van der Schaaf A, van Dijk LV, van den Bergh ACM, Langendijk JA. Development of a prediction model for late urinary incontinence, hematuria, pain and voiding frequency among irradiated prostate cancer patients. PLoS One. 2018;13(7):e0197757.
2. Peisch SF, Van Blarigan EL, Chan JM, Stampfer MJ, Kenfield SA. Prostate cancer progression and mortality: a review of diet and lifestyle factors. World J Urol. 2017;35(6):867–74.
3. Krause M, Dubrovska A, Linge A, Baumann M. Cancer stem cells: Radioresistance, prediction of radiotherapy outcome and specific targets for combined treatments. Adv Drug Deliv Rev. 2017;109:63–73.
4. Ratajczak MZ. Cancer stem cells–normal stem cells "Jedi" that went over to the "dark side". Folia Histochem Cytobiol. 2005;43(4):175–81.
5. Guo Y, Su ZY, Kong AN. Current perspectives on epigenetic modifications by dietary chemopreventive and herbal phytochemicals. Curr Pharmacol Rep. 2015;1(4):245–57.
6. Denis H, Ndlovu MN, Fuks F. Regulation of mammalian DNA methyltransferases: a route to new mechanisms. EMBO Rep. 2011;12(7):647–56.
7. Moore LD, Le T, Fan GP. DNA methylation and its basic function. Neuropsychopharmacol. 2013;38(1):23–38.
8. Hyun K, Jeon J, Park K, Kim J. Writing, erasing and reading histone lysine methylations. Exp Mol Med. 2017;49(4):e324.
9. Berger SL. The complex language of chromatin regulation during transcription. Nature. 2007;447(7143):407–12.
10. Black JC, Van Rechem C, Whetstine JR. Histone lysine methylation dynamics: establishment, regulation, and biological impact. Mol Cell. 2012;48(4):491–507.
11. Ahmed MM, Wang T, Luo Y, Ye S, Wu Q, Guo Z, *et al*. Aldo-keto reductase-7A protects liver cells and tissues from acetaminophen-induced oxidative stress and hepatotoxicity. Hepatology. 2011;54(4):1322–32.
12. Yang Y, Fuentes F, Shu L, Wang C, Pung D, Li W, *et al*. Epigenetic CpG methylation of the promoter and reactivation of the expression of GSTP1 by Astaxanthin in human prostate LNCaP cells. AAPS J. 2017;19(2):421–30.
13. Xie YL, Chu JG, Jian XM, Dong JZ, Wang LP, Li GX, *et al*. Curcumin attenuates lipopolysaccharide/d-galactosamine-induced acute liver injury by activating Nrf2 nuclear translocation and inhibiting NF-kB activation. Biomed Pharmacother. 2017;91:70–7.
14. Nandakumar V, Vaid M, Katiyar SK. (−)-Epigallocatechin-3-gallate reactivates silenced tumor suppressor genes, Cip1/p21 and p16INK4a, by reducing DNA methylation and increasing histones acetylation in human skin cancer cells. Carcinogenesis. 2011;32(4):537–44.
15. Zhang W, Meng Y, Liu N, Wen XF, Yang T. Insights into chemoresistance of prostate Cancer. Int J Biol Sci. 2015;11(10):1160–70.
16. Collins AT, Berry PA, Hyde C, Stower MJ, Maitland NJ. Prospective identification of tumorigenic prostate cancer stem cells. Cancer Res. 2005;65(23):10946–51.
17. Tang SN, Singh C, Nall D, Meeker D, Shankar S, Srivastava RK. The dietary bioflavonoid quercetin synergizes with epigallocathechin gallate (EGCG) to inhibit prostate cancer stem cell characteristics, invasion, migration and epithelial-mesenchymal transition. J Mol Signal. 2010;5:14.
18. Lai CS, Li S, Miyauchi Y, Suzawa M, Ho CT, Pan MH. Potent anti-cancer effects of citrus peel flavonoids in human prostate xenograft tumors. Food Funct. 2013;4(6):944–9.
19. Sergeev IN, Ho CT, Li S, Colby J, Dushenkov S. Apoptosis-inducing activity of hydroxylated polymethoxyflavones and polymethoxyflavones from orange peel in human breast cancer cells. Mol Nutr Food Res. 2007;51(12):1478–84.
20. Chen J, Creed A, Chen AY, Huang H, Li Z, Rankin GO, *et al*. Nobiletin suppresses cell viability through AKT pathways in PC-3 and DU-145 prostate cancer cells. BMC Pharmacol Toxicol. 2014;15:59.

21. Chen C, Ono M, Takeshima M, Nakano S. Antiproliferative and apoptosis-inducing activity of nobiletin against three subtypes of human breast cancer cell lines. Anticancer Res. 2014;34(4):1785–92.
22. Morley KL, Ferguson PJ, Koropatnick J. Tangeretin and nobiletin induce G1 cell cycle arrest but not apoptosis in human breast and colon cancer cells. Cancer Lett. 2007;251(1):168–78.
23. Wesolowska O, Wisniewski J, Sroda-Pomianek K, Bielawska-Pohl A, Paprocka M, Dus D, *et al*. Multidrug resistance reversal and apoptosis induction in human colon cancer cells by some flavonoids present in citrus plants. J Nat Prod. 2012;75(11):1896–902.
24. Xiao H, Yang CS, Li S, Jin H, Ho CT, Patel T. Monodemethylated polymethoxyflavones from sweet orange (*Citrus sinensis*) peel inhibit growth of human lung cancer cells by apoptosis. Mol Nutr Food Res. 2009;53(3):398–406.
25. Li S, Pan MH, Lai CS, Lo CY, Dushenkov S, Ho CT. Isolation and syntheses of polymethoxyflavones and hydroxylated polymethoxyflavones as inhibitors of HL-60 cell lines. Bioorg Med Chem. 2007;15(10):3381–9.
26. Guo S, Wu X, Zheng J, Charoensinphon N, Dong P, Qiu P, *et al*. Anti-inflammatory effect of xanthomicrol, a major colonic metabolite of 5-demethyltangeretin. Food Funct. 2018;9(6):3104–13.
27. Moghaddam G, Ebrahimi SA, Rahbar-Roshandel N, Foroumadi A. Antiproliferative activity of flavonoids: influence of the sequential methoxylation state of the flavonoid structure. Phytother Res. 2012;26(7):1023–8.
28. Zheng J, Song M, Dong P, Qiu P, Guo S, Zhong Z, *et al*. Identification of novel bioactive metabolites of 5-demethylnobiletin in mice. Mol Nutr Food Res. 2013;57(11):1999–2007.
29. Wang Y, Yin JL, Qu XJ, Mu YL, Teng SL. Prostate cancer Lncap stem-like cells demonstrate resistance to the hydros-induced apoptosis during the formation of spheres. Biomed Pharmacother. 2015;74:1–8.
30. Su ZY, Zhang C, Lee JH, Shu L, Wu TY, Khor TO, *et al*. Requirement and epigenetics reprogramming of Nrf2 in suppression of tumor promoter TPA-induced mouse skin cell transformation by sulforaphane. Cancer Prev Res (Phila). 2014;7(3):319–29.
31. Su ZY, Tung YC, Hwang LS, Sheen LY. Blazeispirol a from Agaricus blazei fermentation product induces cell death in human hepatoma Hep 3B cells through caspase-dependent and caspase-independent pathways. J Agric Food Chem. 2011;59(9):5109–16.
32. Zhang C, Su ZY, Khor TO, Shu L, Kong AN. Sulforaphane enhances Nrf2 expression in prostate cancer TRAMP C1 cells through epigenetic regulation. Biochem Pharmacol. 2013;85(9):1398–404.
33. Bott SR, Arya M, Kirby RS, Williamson M. p21WAF1/CIP1 gene is inactivated in metastatic prostatic cancer cell lines by promoter methylation. Prostate Cancer Prostatic Dis. 2005;8(4):321–6.
34. Su ZY, Khor TO, Shu L, Lee JH, Saw CL, Wu TY, *et al*. Epigenetic reactivation of Nrf2 in murine prostate cancer TRAMP C1 cells by natural phytochemicals Z-ligustilide and Radix angelica sinensis via promoter CpG demethylation. Chem Res Toxicol. 2013;26(3):477–85.
35. Lin JC, Wu YC, Wu CC, Shih PY, Wang WY, Chien YC. DNA methylation markers and serum alpha-fetoprotein level are prognostic factors in hepatocellular carcinoma. Ann Hepatol. 2015;14(4):494–504.
36. Shim JH, Su ZY, Chae JI, Kim DJ, Zhu F, Ma WY, *et al*. Epigallocatechin gallate suppresses lung cancer cell growth through Ras-GTPase-activating protein SH3 domain-binding protein 1. Cancer Prev Res (Phila). 2010;3(5):670–9.
37. Dong A, Yoder JA, Zhang X, Zhou L, Bestor TH, Cheng X. Structure of human DNMT2, an enigmatic DNA methyltransferase homolog that displays denaturant-resistant binding to DNA. Nucleic Acids Res. 2001;29(2):439–48.
38. Bikadi Z, Hazai E. Application of the PM6 semi-empirical method to modeling proteins enhances docking accuracy of AutoDock. J Cheminform. 2009;1:15.
39. Charoensinphon N, Qiu P, Dong P, Zheng J, Ngauv P, Cao Y, *et al*. 5-demethyltangeretin inhibits human nonsmall cell lung cancer cell growth by inducing G2/M cell cycle arrest and apoptosis. Mol Nutr Food Res. 2013;57(12):2103–11.
40. Febriansah R, Putri DD, Sarmoko, Nurulita NA, Meiyanto E, Nugroho AE. Hesperidin as a preventive resistance agent in MCF-7 breast cancer cells line resistance to doxorubicin. Asian Pac J Trop Biomed. 2014;4(3):228–33.
41. Shirzad M, Heidarian E, Beshkar P, Gholami-Arjenaki M. Biological effects of hesperetin on interleukin-6/phosphorylated signal transducer and activator of transcription 3 pathway signaling in prostate cancer PC3 cells. Pharm Res. 2017;9(2):188–94.
42. Talmadge JE, Fidler IJ. AACR centennial series: the biology of cancer metastasis: historical perspective. Cancer Res. 2010;70(14):5649–69.
43. Bhardwaj M, Kim NH, Paul S, Jakhar R, Han J, Kang SC. 5-Hydroxy-7-methoxyflavone triggers mitochondrial-associated cell death via reactive oxygen species signaling in human colon carcinoma cells. PLoS One. 2016;11(4):e0154525.
44. Phromnoi K, Reuter S, Sung B, Limtrakul P, Aggarwal BB. A Dihydroxy-pentamethoxyflavone from Gardenia obtusifolia suppresses proliferation and promotes apoptosis of tumor cells through modulation of multiple cell signaling pathways. Anticancer Res. 2010;30(9):3599–610.
45. Zhang X, Song X, Yin S, Zhao C, Fan L, Hu H. p21 induction plays a dual role in anti-cancer activity of ursolic acid. Exp Biol Med (Maywood). 2016;241(5):501–8.
46. Myzak MC, Dashwood WM, Orner GA, Ho E, Dashwood RH. Sulforaphane inhibits histone deacetylase in vivo and suppresses tumorigenesis in Apc-minus mice. FASEB J. 2006;20(3):506–8.
47. Myzak MC, Hardin K, Wang R, Dashwood RH, Ho E. Sulforaphane inhibits histone deacetylase activity in BPH-1, LnCaP and PC-3 prostate epithelial cells. Carcinogenesis. 2006;27(4):811–9.
48. Khan MA, Hussain A, Sundaram MK, Alalami U, Gunasekera D, Ramesh L, *et al*. (−)-Epigallocatechin-3-gallate reverses the expression of various tumor-suppressor genes by inhibiting DNA methyltransferases and histone deacetylases in human cervical cancer cells. Oncol Rep. 2015;33(4):1976–84.
49. Goll MG, Kirpekar F, Maggert KA, Yoder JA, Hsieh CL, Zhang X, *et al*. Methylation of tRNAAsp by the DNA methyltransferase homolog Dnmt2. Science. 2006;311(5759):395–8.
50. Kristiansen G, Pilarsky C, Wissmann C, Stephan C, Weissbach L, Loy V, *et al*. ALCAM/CD166 is up-regulated in low-grade prostate cancer and progressively lost in high-grade lesions. Prostate. 2003;54(1):34–43.
51. Jiao J, Hindoyan A, Wang S, Tran LM, Goldstein AS, Lawson D, *et al*. Identification of CD166 as a surface marker for enriching prostate stem/progenitor and cancer initiating cells. PLoS One. 2012;7(8):e42564.